

Analytical Modeling of Dual Material Junctionless Surrounding Gate MOSFET

S.Archana¹, G.Vallathan², M.Anantha Kumar³

¹scholar, ²associate Professor, ³assistant Professor
^{1,2,3} Ifet College Of Engineering, Villupuram

Abstract-

The conventional MOSFET is heavily affected by the short channel effects. These effects can be reduced by means of multigate MOSFET. But even in multi gate MOSFET, there is a presence of effects such as threshold voltage roll off, drain induced barrier lowering and difficulties due to the fabrication process. To simplify fabrication process, the technology named as junctionless transistors arises. Surrounding gate MOSFET is the promising structure for minimizing the occupied area and also the reduction of power consumption. By considering the benefits of all those existing model, the analytical modeling of Junctionless surrounding gate MOSFET is derived. Also by taking the dual material advantages, a technology named as dual material junctionless surrounding gate MOSFET is proposed and the equation for surface potential is obtained by applying the boundary conditions in Poisson's equation. By using that derived equations, various characteristics and behavior of the device such as surface potential, threshold voltage, and sub-threshold swing were plotted against length, radius, doping concentration using MATLAB software.

Keywords-- Short channel effects (SCE), Junctionless transistors (JL), Surrounding gate transistors (SGT), Dual material gate (DMG), Dual material junctionless surrounding gate MOSFET (DMJLSGT)

I. INTRODUCTION

The scaling of conventional MOSFET is suffered by short channel effects when we reduce the channel length of the transistor. The transistors with junction requires the steep doping profile for the source and drain end and also put challenges in the thermal budget. Hence to minimize the short channel effects, thermal budgets and disadvantages due to junctions, there is an emergence of the newly devised model termed as junctionless transistor (JL). In which there is no abrupt junctions for source and the drain side, resulting in improved SCEs performance, better scaling and reduced thermal budget. The JL is different from the traditional surrounding gate transistors in which source, drain, channel having the same doping concentration i.e. P+P+P+ or N+N+N+. The performance is also improved by maximizing the extension of the gate control deeper into the source and drain region [1-3]. Wherever the surrounding gate transistors (SGT) are proposed to improve the

electrostatic controllability of the gate [4-5]. Dual material gate (DMG) has two metal gates termed as control gate and screening gate. The work function of the gate metal 1 is higher in comparison with the work function of gate metal 2. The potential and field distributions of the channel are controlled by adjusting the work functions of the gate metals. There are variety of advantages are there for the dual material gate such as its carrier efficiency is high, improved drain output resistance and higher transconductance in comparison with the single material gate (SMG) [6-9]. Hence by combining all the advantages of JL, SGT and DMG, we proposed a new model termed as dual material junctionless surrounding gate MOSFET (DMJSGT). For the proposed model, the expression for surface potential, threshold voltage and sub threshold swing is derived. These derived parameters are stimulated using MATLAB software.

II. DEVICE STRUCTURE

The device structure of DMJSGT comprises of source, channel, dual material gate and drain. In which the source, channel and gate is doped uniformly (N+). P+ polysilicon acts as a gate material. L_1 and L_2 are the length of gate metals 1 and 2. The total channel length is given by $L_1 + L_2$. The work function of gate metal 1 is higher than the work function of gate metal 2 i.e. the threshold voltage of metal 1 ($V_{T(M1)}$) is higher than the threshold voltage of metal 2 ($V_{T(M2)}$). The work function difference between these two gate metals is important in determine the device characteristics. The threshold voltage (V_T) and work function (ϕ) is given by the relation $\Delta V_T = S \Delta \phi$ $S=1$ for silicon MOSFET [10].

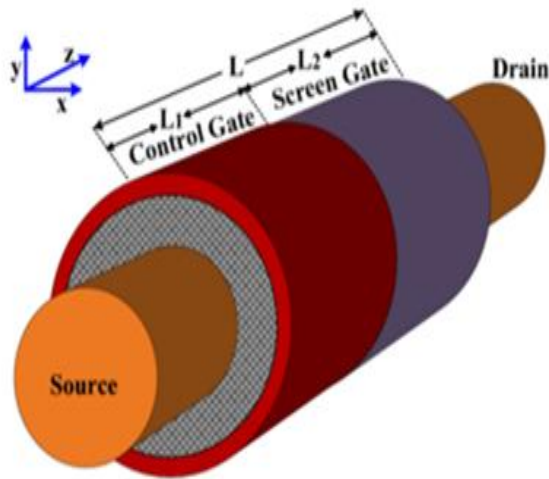


Figure 1: Structure of DMJSGT

III. MODEL DERIVATION

A. Boundary Conditions

The surface potential at the interface of two dissimilar gate materials is continuous

$$\phi_1(L_1, 0) = \phi_2(L_1, 0)$$

- 1) The variation of channel potential at the surface ($\rho = t_{si}/2$) for gate-1

$$\frac{d\phi}{d\rho} = \frac{-\epsilon_{ox} \phi_s(z) - V_{gs} + \phi_{MS1}}{\epsilon_{si} t'_{ox}}$$

where $t'_{ox} = \rho \ln(1 + t_{ox}/\rho)$

- 2) The variation of channel potential at the surface ($\rho = t_{si}/2$) for gate-2

$$\frac{d\phi}{d\rho} = \frac{-\epsilon_{ox} \phi_s(z) - V_{gs} + \phi_{MS2}}{\epsilon_{si} t'_{ox}}$$

where $t'_{ox} = \rho \ln(1 + t_{ox}/\rho)$

- 3) The potential at the source and drain end, under material 1 and material 2 are

- i. $\phi(L_1) = V_{DS} - (V_{GS} - \phi_{MS1})$

- ii. $\phi(L_2) = (V_{GS} - \phi_{MS2})$

B. Surface Potential Model

In subthreshold region, where the silicon layer is fully depleted, the Poisson's equation is given by

$$\frac{d^2}{dz^2} \phi(0, z) - \frac{1}{\lambda^2} (\phi(0, z)) = \frac{-qN_D}{\epsilon_{si}} - \frac{(V_{gs} - \phi_{MS})}{\lambda^2}$$

Taking $\frac{-qN_D}{\epsilon_{si}} - \frac{(V_{gs} - \phi_{MS})}{\lambda^2}$ as β , Poisson equation for gate material-1 and gate material-2 can be given by

$$\frac{d^2}{dz^2} \phi(0, z) - \frac{1}{\lambda^2} (\phi(0, z)) = \beta_1 \quad (1)$$

$$\frac{d^2}{dz^2} \phi(0, z) - \frac{1}{\lambda^2} (\phi(0, z)) = \beta_2 \quad (2)$$

Upon using parabolic approximation, the solution for equation (1) and (2) can be given by

$$\phi_1(z) = Ae^{-z/\lambda} + Be^{z/\lambda} + (V_{gs} - \phi_{MS1}) + \frac{qN_D}{\epsilon_{si}} \lambda^2 \quad (3)$$

$$\phi_2(z) = Ae^{-z/\lambda} + Be^{z/\lambda} + (V_{gs} - \phi_{MS2}) + \frac{qN_D}{\epsilon_{si}} \lambda^2 \quad (4)$$

Using the defined boundary conditions, the arbitrary constants can be found and is substituted in equation (3) and (4) gives us

Surface potential under material-1

$$\phi_1(0, z) = (V_{gs} - \phi_{MS1}) + \frac{qN_D}{\epsilon_{si}} \lambda^2 + \left[\frac{A + B}{\sinh\left(\frac{L_1}{\lambda}\right)} \right]$$

where

$$A = \left(V_{DS} - (V_{gs} - \phi_{MS1}) - \frac{qN_D}{\epsilon_{si}} \lambda^2 \right) \sinh\left(\frac{z}{\lambda}\right)$$

$$B = \left(-(V_{gs} - \phi_{MS1}) - \frac{qN_D}{\epsilon_{si}} \lambda^2 \right) \sinh\left(\frac{L_1 - z}{\lambda}\right)$$

Surface potential under material-2

$$\phi_2(0, z) = (V_{gs} - \phi_{MS1}) + \frac{qN_D}{\epsilon_{si}} \lambda^2 + \left[\frac{A + B}{\sinh\left(\frac{L_2}{\lambda}\right)} \right]$$

where

$$A = \left(V_{DS} - (V_{gs} - \phi_{MS1}) - \frac{qN_D}{\epsilon_{si}} \lambda^2 \right) \sinh\left(\frac{L_1 + L_2 - z}{\lambda}\right)$$

$$B = \left(-(V_{gs} - \phi_{MS1}) - \frac{qN_D}{\epsilon_{si}} \lambda^2 \right) \sinh\left(\frac{L_2 - z}{\lambda}\right)$$

C. Threshold Voltage Model

The threshold voltage is the voltage required to form a channel and it is maximum at which the surface potential is minimum and when it equals $2\phi_F$. The channel position at which the potential is minimum, can be determined by

$$\frac{d}{dz} [\phi(0, z)]_{z_{min}} = 0$$

By solving the above differential equation, we get,

$$z_{min} = \frac{\lambda}{2} \ln \left\{ \frac{C_1 - C_2 e^{L/\lambda}}{C_2 e^{-L/\lambda} - C_1} \right\}$$

$$C_1 = \left(\frac{qN_D}{\epsilon_{si}} \lambda^2 + (V_{gs} - \phi_{MS}) - V_{ds} \right), C_2 = \left(\frac{qN_D}{\epsilon_{si}} \lambda^2 + (V_{gs} - \phi_{MS}) \right)$$

Then the threshold voltage is given by

$$V_{th} = \phi_{MS} + \frac{qN_D}{\epsilon_{si}} \lambda^2 - \left[\frac{2\phi_F \sinh\left(\frac{L}{\lambda}\right) - V_{ds} \sinh\left(\frac{z_{min}}{\lambda}\right)}{\sinh\left(\frac{L}{\lambda}\right) - \sinh\left(\frac{z_{min}}{\lambda}\right) - \sinh\left(\frac{L-z_{min}}{\lambda}\right)} \right]$$

D. Subthreshold Swing

The threshold voltage variation along with channel length (sub-threshold swing) can be given as

$$\frac{\partial V_{th}}{\partial L} = \frac{UV' - VU'}{V^2}$$

Where $U = 2\phi_F \sinh\left(\frac{L}{\lambda}\right) - V_{ds} \sinh\left(\frac{z_{min}}{\lambda}\right)$
 $U' = \frac{2\phi_F}{\lambda} \cosh\left(\frac{L}{\lambda}\right) - \frac{1}{\lambda} \frac{\partial z_{min}}{\partial L} V_{ds} \sinh\left(\frac{z_{min}}{\lambda}\right)$
 $V = \sinh\left(\frac{L}{\lambda}\right) - \sinh\left(\frac{z_{min}}{\lambda}\right) - \sinh\left(\frac{L-z_{min}}{\lambda}\right)$
 $V' = \left[\frac{1}{\lambda} \cosh\left(\frac{L}{\lambda}\right) - \frac{1}{\lambda} \frac{\partial z_{min}}{\partial L} \cosh\left(\frac{z_{min}}{\lambda}\right) \right]$
 $\quad \left[-\frac{1}{\lambda} \left(1 - \frac{\partial z_{min}}{\partial L}\right) \cosh\left(\frac{L-z_{min}}{\lambda}\right) \right]$

Where $\frac{\partial z_{min}}{\partial L} = \frac{-1}{2} \left[\xi \left(\frac{e^{L/\lambda}}{C_1 - C_2 e^{L/\lambda}} - \frac{e^{-L/\lambda}}{C_2 e^{-L/\lambda} - C_1} \right) \right]$
 $\xi = (V_{gs} - \phi_{MS}) + \frac{qN_D}{\epsilon_{si}} \lambda^2$

IV. RESULTS AND DISCUSSION

In this results and discussion section, the surface potential variation along the channel position for DMJLSGT is stimulated using MATLAB software. The threshold voltage variation for different doping concentration, silicon body radius are viewed graphically. With these graphical results, it has been realized that the DMJLSGT exhibits better performance than the single material gate transistors.

A. Surface Potential Vs Channel Position

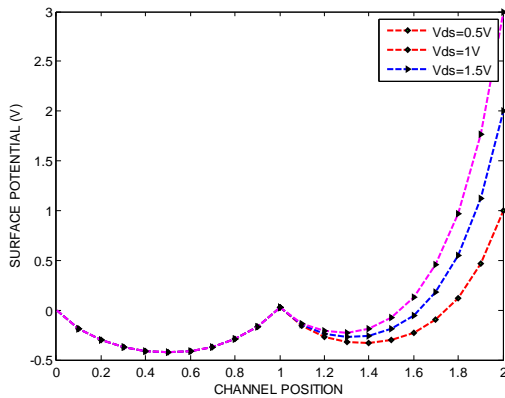
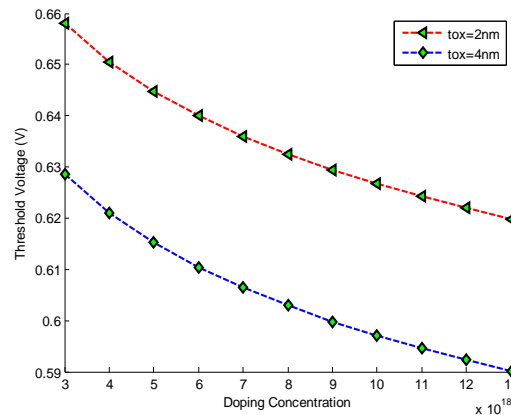


Figure 2 : Output for Surface Potential vs Channel Position

Figure 2 shows the Variation of Surface potential of JLDGT with its channel position for $V_{DS}=0.5V$, $V_{DS}=1V$ and $V_{DS}=1.5V$. From figure 2 it has been inferred that there is no variation in Material 1 when compared to Material 2. Because the Material 2 is present in Drain side and hence there is variation when we apply V_{DS} . Since the material which is having large work function, only determines the threshold voltage of the device, so the threshold voltage model for dual-material gate is as same as single material gate.

(8)

B. Threshold Voltage Vs Doping Concentration



(9)

Figure 3: Output for Threshold Voltage vs Doping Concentration

Figure 3 shows the Output for Threshold Voltage vs Doping Concentration for $tox=2nm$ and $tox=4nm$. The device parameters used here are $L=20nm$, $R=3nm$ and $V_{DS}=0.5V$.

C. Threshold Voltage Vs Channel Length

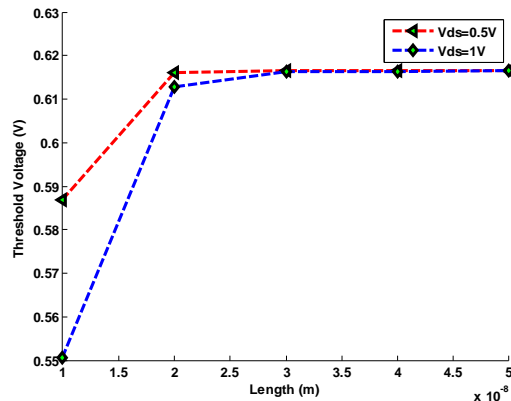


Figure 4 : Output for Threshold Voltage vs Channel Length

Figure 4 shows the Output for Threshold Voltage vs Channel Length for $V_{DS}=0.5v$ and $V_{DS}=0.5v$. The device parameters used are $R=3nm$, $N_D=10^{19}cm^{-3}$.

From figure 4 it can be said that the variation in length upto 20nm, causes a vast variation in V_{th} .

So the length of the device can be chosen as 20 nm upto this result. Length which is larger than 20 nm is safer for good threshold voltage

D. Subthreshold Swing Vs Channel Length

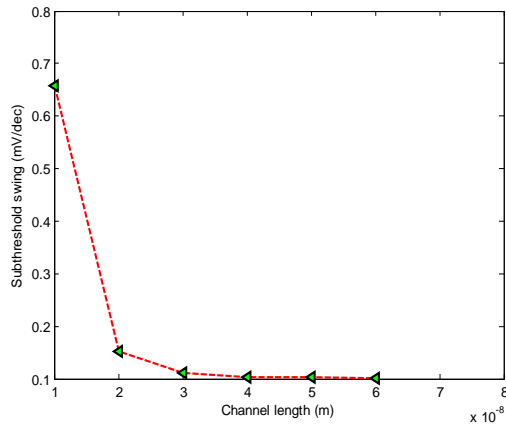


Figure 5: Output for Subthreshold Swing vs Channel Length

Figure 5 shows the Variation of Subthreshold swing of Junctionless DMDG Transistor with channel length. From figure 5 it can be observed that the devices with $L > 30\text{nm}$, the values of S are quite satisfactory.

V. CONCLUSION

In this present work, the analytical model for the dual material junctionless surrounding gate MOSFET(DMJSGLT) is proposed. Various characteristics and behavior of the device such as surface potential, threshold voltage, subthreshold swing were plotted against length, radius, doping concentration using MATLAB software. It has been concluded that the DMJSGT MOSFET is highly immune to short channel effects compared to SMJSGT MOSFET.

REFERENCES

[1] CW. Lee, A. Afzalian, N. Dehdashti Akhavan, R. Yan, I. Ferain, JP. Colinge, "Junctionless multigate field-effect transistor", Applied Physics Letters, Vol. 94, pp. 053511:1-2, 2009

[2] C.W. Lee, I. Ferain, A. Afzalian, R. Yan, N. Dehdashti Akhavan, P. Razavi, J.P. Colinge, "Performance estimation of junctionless multigate transistors", Solid-State Electronics, Vol. 54, pp. 97-103, 2010

[3] JP Colinge, CW Lee, A. Afzalian, N. Dehdashti Akhavan, R. Yan, I. Ferain, P. Razavi, B. O'Neill, A. Blake, M. White, AM Kelleher, B. McCarthy, R. Murphy, "Nanowire transistors without junctions", Nature Nanotechnology, Vol. 5, No. 3, pp. 225-229, 2010

[4] Y.cui, Z.zhong, D.wang, W.wang, and C. M. liebar, "High performance silicon nanowire FET", Nano Lett., vol. 3, no. 2, pp. 149-152, 2003

[5] N. Singh, A. Agarwal, L. K. Bera, T. Y. Liow, R. Yang, S. C. Rustagi, et al., "High performance fully depleted silicon nanowire gate all around CMOS devices" IEEE electr device ,vol 27, nio 5, pp.383-386,may 2006

[6] J.-P. Colinge, C.-W. Lee, A. Afzalian, N. D. Akhavan, R. Yan, I. Ferain, et al., "Nanowire transistors without

junctions," Nat. Nanotechnol.,vol. 5, no. 3, pp. 225–229, Mar. 2010.

[7] C.-W. Lee, A. N. Nazarov, I. Ferain, N. D. Akhavan, R. Yan, P. Razavi, et al., "Low subthreshold slope in junctionless multigate transistor," Appl. Phys. Lett., vol. 96, no. 10, pp. 102106-1–102106-3, Mar. 2010.

[8] C.-W. Lee, I. Ferain, A. Afzalian, R. Yan, N. D. Akhavan, P. Razavi, et al., "Performance estimation of junctionless multigate transistors," Solid State Electron., vol. 54, no. 2, pp. 97–103, Feb. 2010.

[9] C.-W. Lee, I. Ferain, A. Afzalian, R. Yan, N. D. Akhavan, P. Razavi, et al., "Performance estimation of junctionless multigate transistors," Solid State Electron., vol. 54, no. 2, pp. 97–103, Feb. 2010

[10] Ratul K. Baruah, Member, IEEE, and Roy P. Paily, Member, IEEE," A Dual-Material Gate Junctionless Transistor With High-k Spacer for Enhanced Analog Performance", vol. 61, no. 1, January 2014